Supplement of Atmos. Chem. Phys., 25, 11919–11933, 2025
https://doi.org/10.5194/acp-25-11919-2025-supplement

Atmospheric Chemistry and Physics
Open Access
EGU

Supplement of

Bioaerosols as indicators of central Arctic ice nucleating particle sources

Kevin R. Barry et al.

Correspondence to: Kevin R. Barry (kevin.barry@colostate.edu)

Section S1

INP concentrations reported herein for filter-based collections and processing are typically higher than previously published MOSAiC INP concentrations based on DRUM size-segregated samples (Fig. S7: Creamean et al., 2022). For the DRUM data that represent an integration of all size stages (0.15-12 μm), seasonally-averaged concentrations for INPs active at -15 °C were as follows: fall=$1.8x10^{-5}$ L^{-1}; winter=$6.1x10^{-5}$ L^{-1}; spring=$6.3x10^{-5}$ L^{-1}; summer=$1.1x10^{-3}$ L^{-1}. Seasonal averages for the polycarbonate filters were $4.4x10^{-3}$ L^{-1}, $1.1x10^{-3}$ L^{-1}, $1.1x10^{-3}$ L^{-1}, and 2.4 $x10^{-1}$ L^{-1}. Similar seasonality trends were detected in both data sets, although with 1-3 orders of magnitude lower concentrations for the integrated DRUM samples for INP activation temperatures warmer than -20 °C (Fig. S7). There are several potential explanations for the discrepancies observed, such as differences in sampling inlets (Creamean et al., 2022), aerosol collection size range, inefficient collection (e.g. potential particle bounce in cold environments) and removal of particles during analysis, and certain samples (and stages) subjected to a different cooling rate than others during analysis of DRUM samples (Between 0-8 °C min^{-1}). This different cooling rate was a function of some DRUM samples (primarily spring and summer) being analyzed in a different laboratory with a ~15-20 °C colder ambient temperature. The sample integration time differences (24- versus 72-hour) could result in short term concentration discrepancies but should not influence the seasonal averages. Comparisons with two other Arctic ground studies that made measurements at the same time as MOSAiC (Li et al., 2022; Sze et al., 2023) revealed much better agreement with the polycarbonate filters analyzed with the IS (Fig. S7), which gives confidence in this dataset as representative of both the central and wider Arctic basin. Comparison tests and investigations of this result are ongoing. When DRUM samples were run on the IS, the agreement was generally much better to the total aerosol filters, suggesting measurement techniques account for at least some of the discrepancies (Fig. S7). Overall, the INPs from the DRUM and cold plate analysis should be viewed as a lower bound or subset of observed total aerosol INPs. The use of only the total aerosol INPs for future studies is recommended as it is more representative.

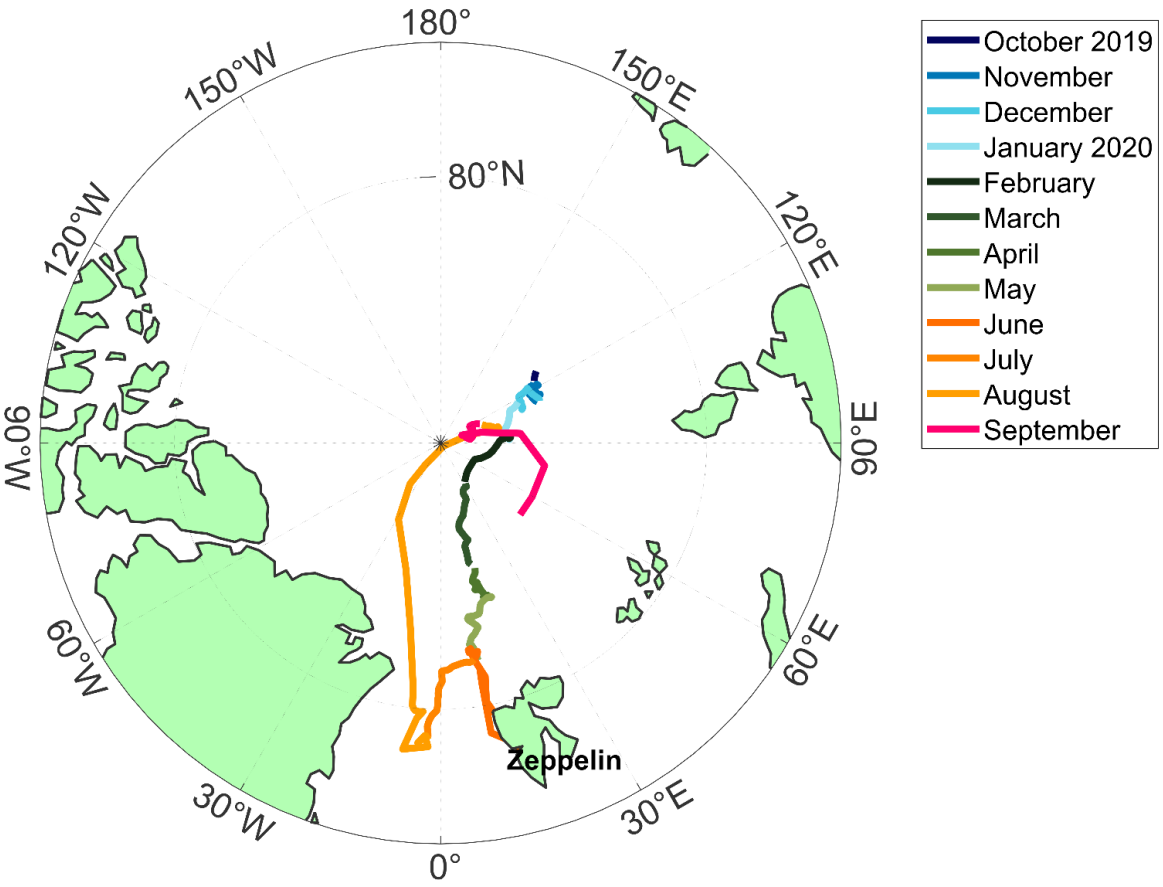

Figure S1: Ship track of the R/V *Polarstern* from 10/27/2019-9/25/2025. Created with MATLAB M_Map (Pawlowicz, 2020).

25

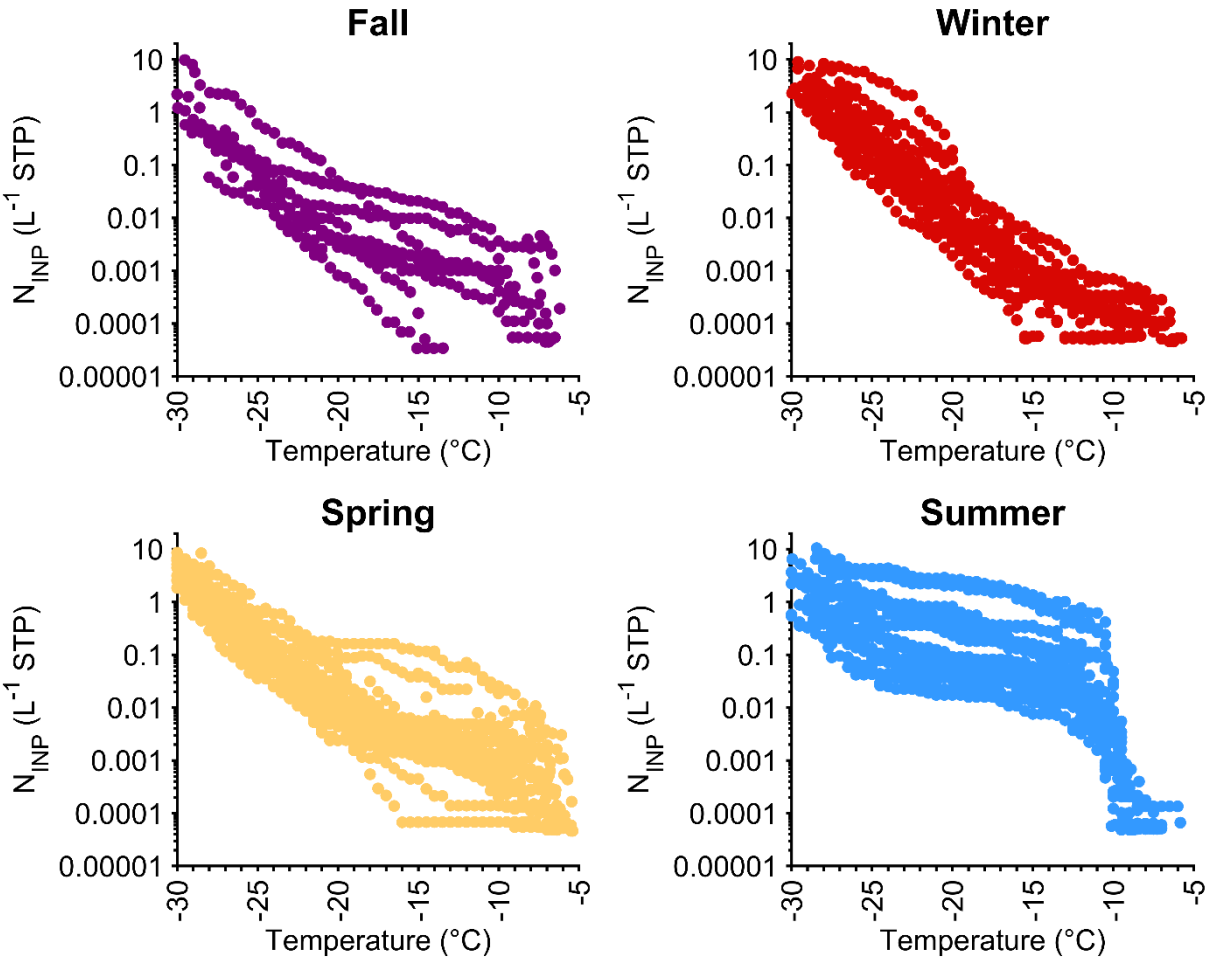

Figure S2: Cumulative INP-temperature spectra, colored by season. Fall (Purple: September, October, November), Winter (Red: December, January, February), Spring (Yellow: March, April, May), Summer (Blue: June, July, August).

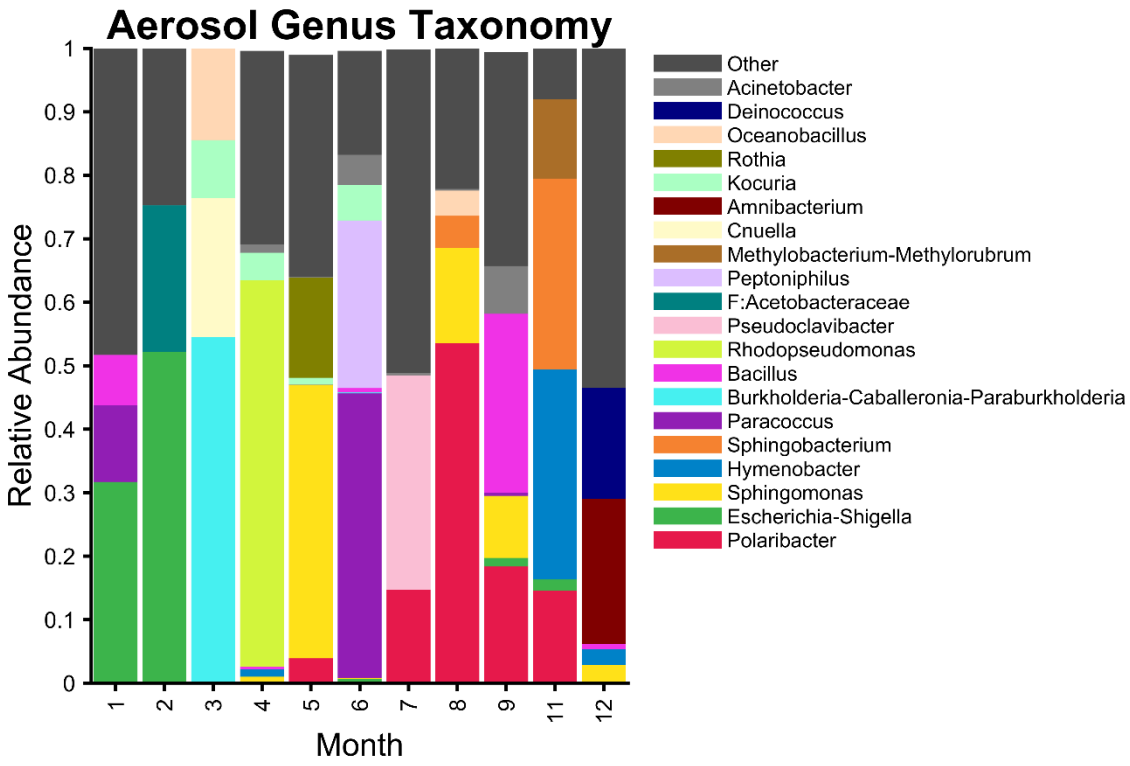

Figure S3: Pooled monthly aerosol bacterial taxonomy plot, colored by the top 20 genera. Any taxa contributing less than 0.1% relative abundance were excluded from the analysis.

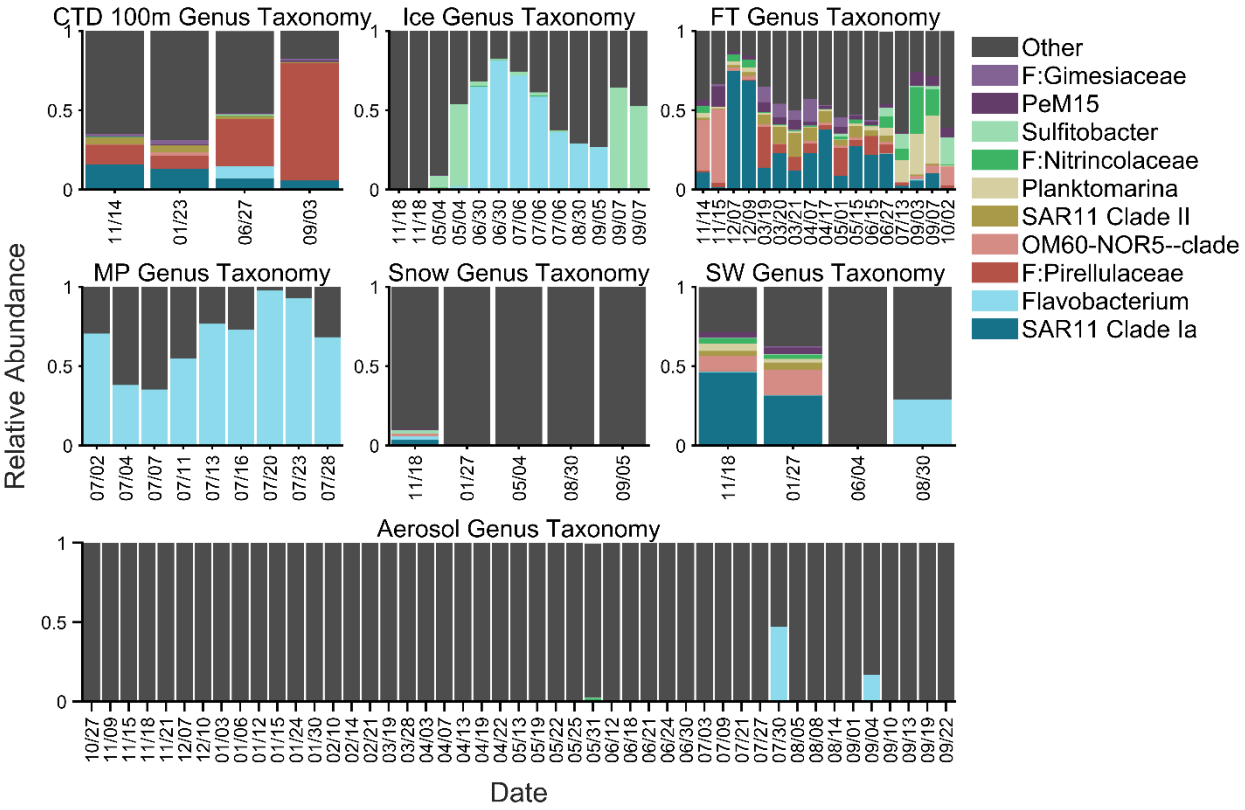

Figure S4: Bacterial genus level relative abundance taxonomy for the different potential local sources and aerosol as a function of month collected. FT=Flowthrough; MP=Melt pond; SW=Lead water. The samples are colored by the top 10 genera for all source samples combined, with family (F) given if not resolved at the genus level.

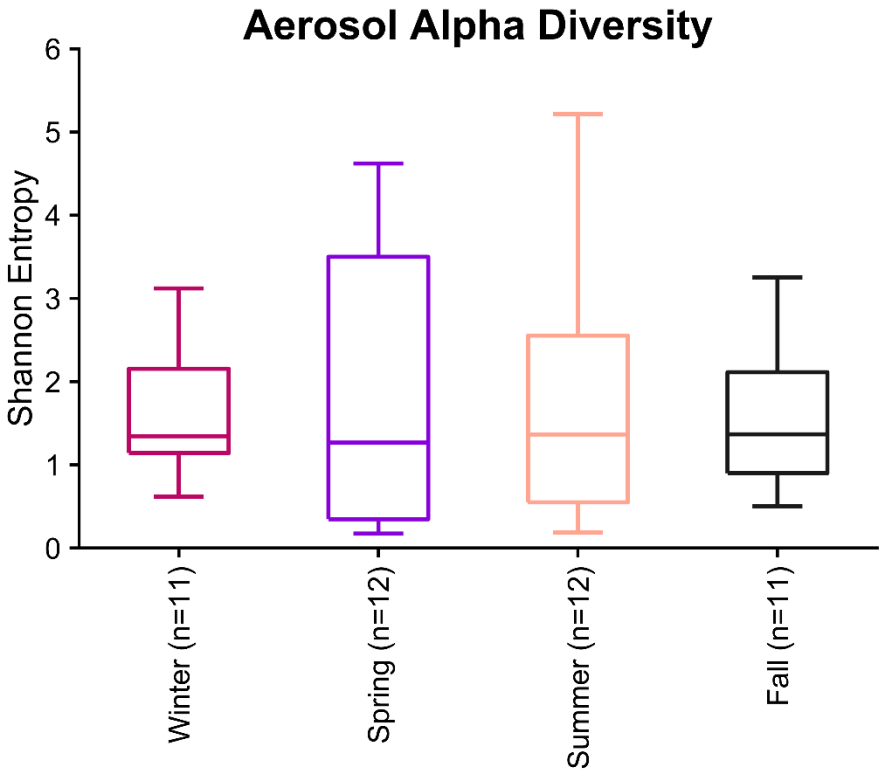

Figure S5: Alpha diversity (Shannon entropy) as a function of season for the bacterial aerosol samples. Number of samples (n=) is given.

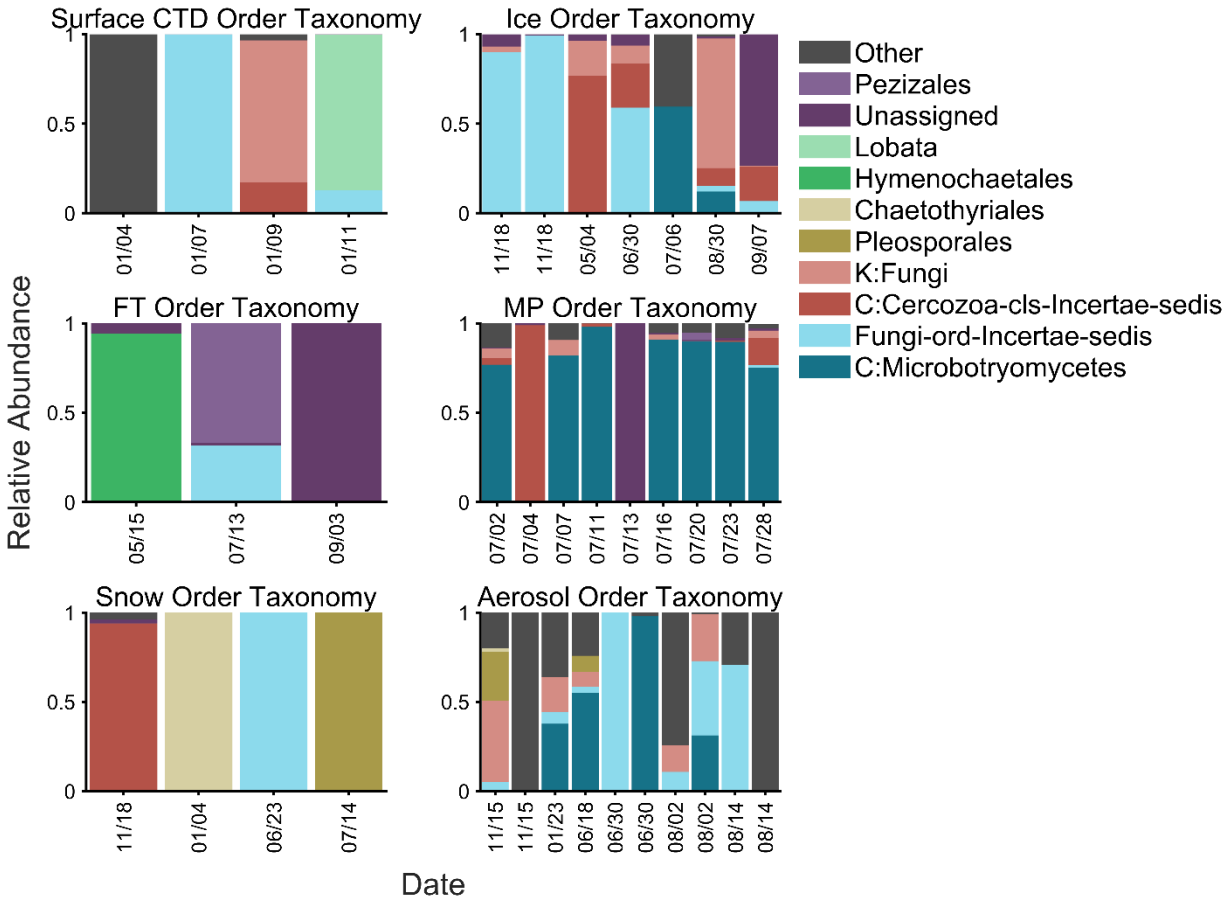

Figure S6: Fungal order level relative abundance taxonomy for the different potential local sources and aerosol as a function of month collected. FT=Flowthrough; MP=Melt pond; SW=Lead water. The samples are colored by the top 10 genera for all sources combined, with kingdom (K), phylum (P), and class (C) given if not resolved at the genus level.

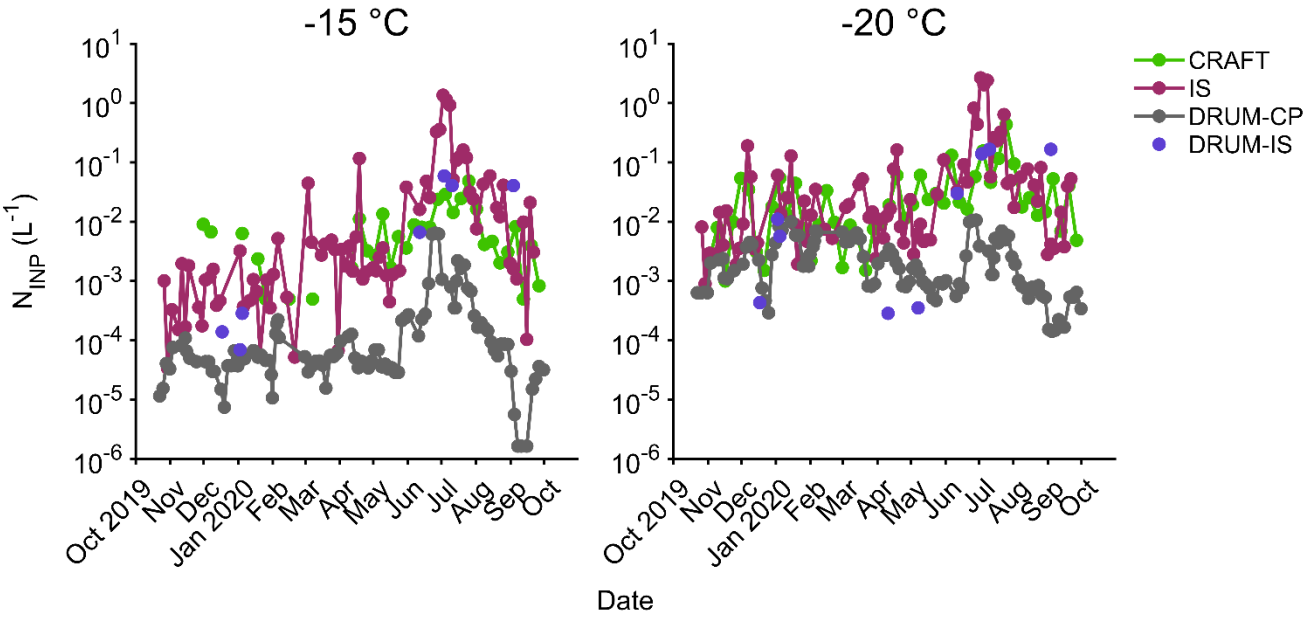

Figure S7: INP concentration time series during the MOSAiC campaign at -15 °C (left) and -20 °C (right). CRAFT (green) refers to data take at Zeppelin Observatory at Svalbard (Pereira Freitas et al., 2023; Tobo et al., 2024); IS (purple) refers to filter samples analyzed with the Ice Spectrometer; DRUM-CP (gray) refers to the total DRUM samples analyzed on the cold plate; and DRUM-IS (blue) refers to select total DRUM samples analyzed on the Ice Spectrometer. Size resolved aerosol for INP analyses were collected with a 4-stage Davis Rotating-drum Unit for Monitoring cascade impactor (DRUM) with the AOS inlet (Creamean et al., 2022).

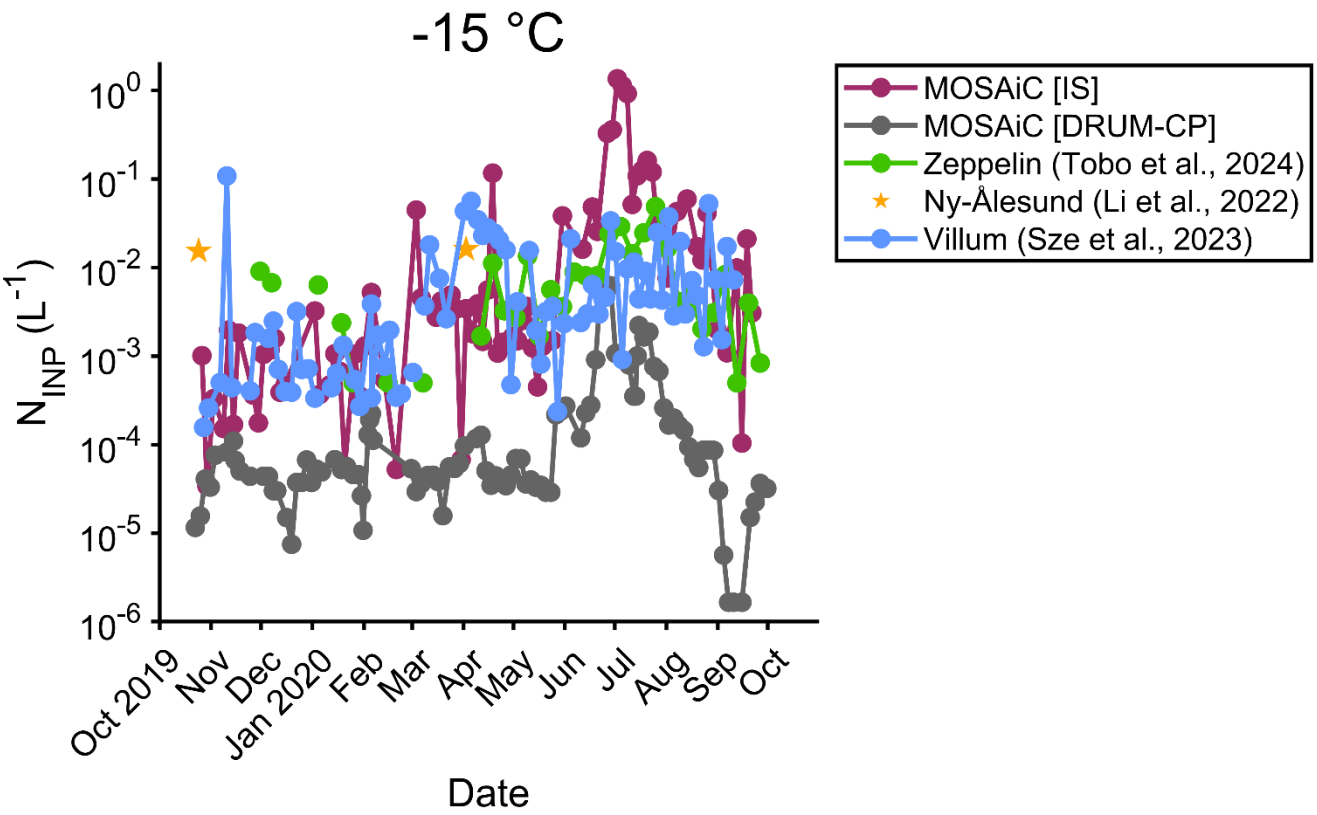

Figure S8: INP concentration time series during the MOSAiC campaign time period at -15 °C. MOSAiC [IS] (purple) refers to MOSAiC filter samples analyzed with the Ice Spectrometer; MOSAiC [DRUM-CP] (gray) refers to the total MOSAiC DRUM samples analyzed on the cold plate (Creamean et al., 2022); Zeppelin (green) refers to data take at Zeppelin Observatory at Svalbard (Pereira Freitas et al., 2023; Tobo et al., 2024); Ny-Ålesund (yellow) refers to the seasonally averaged data from Li et al. (2022) collected at Ny-Ålesund; Villum (blue) refers to the filter data from Sze et al. (2023) collected at Villum Research Station.

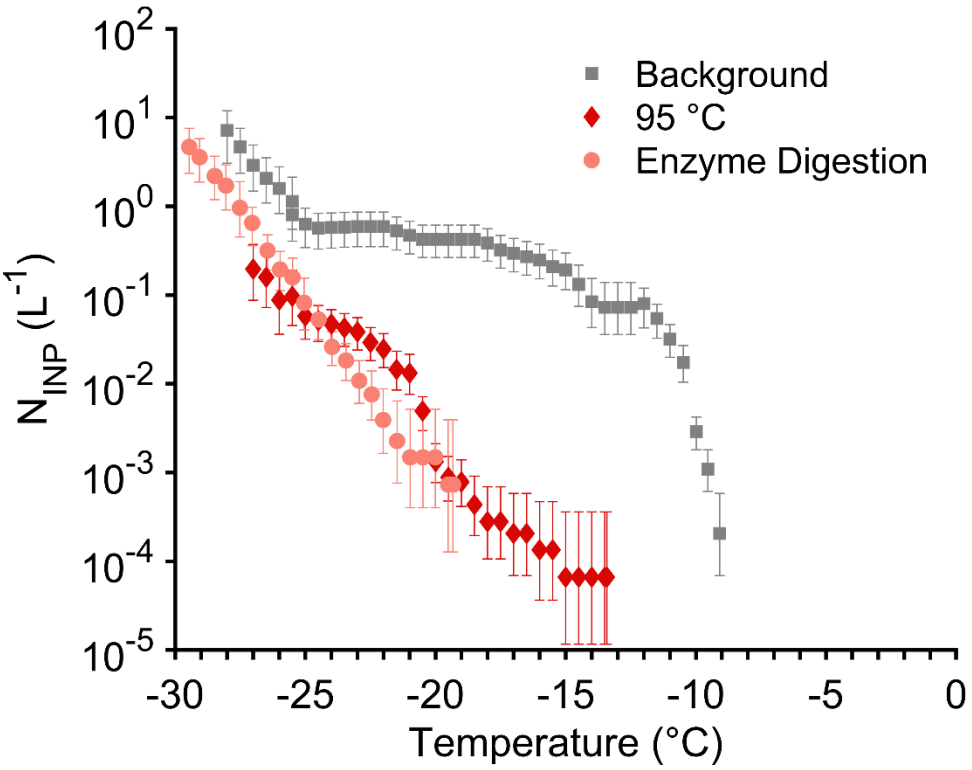

Figure S9: Comparison between heating (red diamonds) and an enzymatic (MetaPolyzyme: Sigma, and Proteinase-K) digestion (salmon circles) of the filter suspension for 6/24-27/2020.

Type	Collection Date (UTC)	Latitude (°N)	Longitude (°E)	Depth (m)
Snow	10/25/2019 12:00	85.436900	128.146900	0.26
FT	11/14/2019 6:30	86.188309	118.416527	11
CTD	11/14/2019 12:00	86.153053	118.109711	100
CTD	11/14/2019 12:00	86.153053	118.109711	10
CTD	11/14/2019 12:00	86.153053	118.109711	200
CTD	11/14/2019 12:00	86.153053	118.109711	20
CTD	11/14/2019 12:00	86.153053	118.109711	2
FT	11/15/2019 12:00	86.174263	118.245308	11
Ice	11/18/2019 12:00	85.849571	120.581451	Bottom 0-5 cm
Ice	11/18/2019 12:00	85.849571	120.581451	Bottom 5-10 cm
Snow	11/18/2019 12:00	85.849571	120.581451	0
SW	11/18/2019 12:00	85.849571	120.581451	0
CTD	12/6/2019 12:00	86.140556	122.196701	10

FT	12/7/2019 10:00	86.161652	122.141006	11
FT	12/9/2019 9:30	86.401390	120.931358	11
CTD	1/23/2020 12:00	87.446587	94.088547	100
CTD	1/23/2020 12:00	87.446587	94.088547	10
CTD	1/23/2020 12:00	87.446587	94.088547	200
CTD	1/23/2020 12:00	87.446587	94.088547	20
CTD	1/23/2020 12:00	87.446587	94.088547	2
CTD	1/23/2020 12:00	87.446587	94.088547	50
CTD	1/23/2020 12:00	87.446587	94.088547	75
Snow	1/27/2020 12:00	87.445847	95.670288	0
SW	1/27/2020 12:00	87.445847	95.670288	0
FT	3/19/2020 19:38	86.466080	13.943270	11
FT	3/20/2020 11:57	86.330116	14.791050	11
FT	3/21/2020 18:42	86.246986	15.426960	11
Snow	3/22/2020 12:00	86.230000	15.751200	0.215-0.24
FT	4/7/2020 14:58	84.496758	14.549860	11
CTD	4/17/2020 12:00	84.409119	13.652770	2
CTD	4/17/2020 12:00	84.409119	13.652770	20
FT	4/17/2020 18:58	84.428001	13.761420	11
FT	5/1/2020 17:30	83.922569	17.615120	11
Ice	5/4/2020 12:00	83.886208	18.240580	Top 0-10 cm
Ice	5/4/2020 12:00	83.886009	18.314541	Top 30-40 cm
Snow	5/4/2020 12:00	83.886208	18.240580	0
SW	5/4/2020 12:00	83.886208	18.240580	0
FT	5/15/2020 16:30	83.392342	9.178190	11
FT	6/15/2020 19:10	82.218620	8.210060	11
Snow	6/23/2020 12:00	81.998700	9.696600	0.3-0.32
CTD	6/27/2020 12:00	81.955391	9.903160	100
CTD	6/27/2020 12:00	81.955391	9.903160	10
CTD	6/27/2020 12:00	81.955391	9.903160	2
CTD	6/27/2020 12:00	81.955391	9.903160	50
CTD	6/27/2020 12:00	81.955391	9.903160	NA
CTD	6/27/2020 12:00	81.955391	9.903160	150
FT	6/27/2020 16:30	81.918716	9.770960	11
Ice	6/30/2020 12:00	81.783981	8.948390	Bottom 0-5 cm
Ice	6/30/2020 12:00	81.783981	8.948390	Bottom 5-10 cm
MP	7/2/2020 12:00	NA	NA	0
MP	7/4/2020 12:00	NA	NA	0
Ice	7/6/2020 12:00	81.674088	5.190190	NA

Ice	7/6/2020 12:00	81.673447	5.171660	Bottom 5-10 cm
Ice	7/6/2020 12:00	81.673447	5.171660	Bottom 0-5 cm
MP	7/7/2020 12:00	NA	NA	0
MP	7/11/2020 12:00	NA	NA	0
MP	7/13/2020 12:00	NA	NA	0
FT	7/13/2020 21:02	81.406662	0.257950	11
CTD	7/16/2020 12:00	81.230972	0.298100	2
CTD	7/16/2020 12:00	81.230972	0.298100	11
MP	7/16/2020 12:00	NA	NA	0
MP	7/20/2020 12:00	NA	NA	0
MP	7/23/2020 12:00	NA	NA	0
MP	7/28/2020 12:00	NA	NA	0
Lead Ice	8/30/2020 12:00	NA	NA	0
SW	8/30/2020 12:00	NA	NA	0
Snow	8/30/2020 12:00	NA	NA	0
CTD	9/3/2020 12:00	88.560738	119.607590	100
CTD	9/3/2020 12:00	88.560738	119.607590	10
CTD	9/3/2020 12:00	88.560738	119.607590	200
CTD	9/3/2020 12:00	88.560738	119.607590	2
CTD	9/3/2020 12:00	88.560738	119.607590	50
CTD	9/3/2020 12:00	88.560738	119.607590	20
FT	9/3/2020 12:23	88.602692	120.106117	11
Lead Ice	9/5/2020 12:00	NA	NA	0
Snow	9/5/2020 12:00	NA	NA	0
Ice	9/7/2020 12:00	88.722420	112.059280	Top 0-10 cm
Ice	9/7/2020 12:00	88.722420	112.059280	Top 10-20 cm
FT	9/7/2020 13:30	88.688126	111.565254	11
FT	10/2/2020 12:00	NA	NA	11

Table S1: List of potential source samples sequenced with Type (FT=Flowthrough seawater samples; CTD=seawater samples collected on a Conductivity, Temperature, and Depth rosette; SW=Surface or lead seawater samples; MP=Melt pond freshwater samples); Source tracking category; Collection date in UTC (12:00 given if no specific time recorded); Collection latitude in degrees, Collection longitude in degrees; and approximate collection depth in meters. Not available (NA) is indicated, and a default time of "12:00" is given if one was not recorded.

observations of aerosols capable of ice formation in central Arctic clouds, Nat. Commun., 13(1), 3537, https://doi.org/10.1038/s41467-022-31182-x, 2022.

Daily, M. I., Tarn, M. D., Whale, T. F., and Murray, B. J.: An evaluation of the heat test for the ice-nucleating ability of minerals and biological material, Atmos. Meas. Tech., 15(8), 2635–2665, https://doi.org/10.5194/amt-15-2635-2022, 2022.

DeMott, P. J., Swanson, B. E., Creamean, J. M., Tobo, Y., Hill, T. C. J., Barry, K. R., Beck, I. F., Frietas, G. P., Heslin-Rees, D., Lackner, C. P., Schmale, J., Krejci, R., Zieger, P., Geerts, B., and Kreidenweis, S. M.: Ice nucleating particle sources and transports between the Central and Southern Arctic regions during winter cold air outbreaks, Elem. Sci. Anth., 13(1), 00063, https://doi.org/10.1525/elementa.2024.00063, 2025.

Hill, T. C. J., DeMott, P. J., Tobo, Y., Fröhlich-Nowoisky, J., Moffett, B. F., Franc, G. D., and Kreidenweis, S. M.: Sources of organic ice nucleating particles in soils, Atmos. Chem. Phys., 16(11), 7195–7211, https://doi.org/10.5194/acp-16-7195-2016, 2016.

Li, G., Wieder, J., Pasquier, J. T., Henneberger, J., and Kanji, Z. A.: Predicting atmospheric background number concentration of ice-nucleating particles in the Arctic, Atmos. Chem. Phys., 22(21), 14441–14454. https://doi.org/10.5194/acp-22-14441-2022, 2022.

Pawlowicz, R.: "M_Map: A mapping package for MATLAB", version 1.4m, [Computer software], available online at www.eoas.ubc.ca/~rich/map.html, 2020.

Pereira Freitas, G., Adachi, K., Conen, F., Heslin-Rees, D., Krejci, R., Tobo, Y., Yttri, K. E., and Zieger, P.: Regionally sourced bioaerosols drive high-temperature ice nucleating particles in the Arctic, Nat. Commun., 14(1), 5997, https://doi.org/10.1038/s41467-023-41696-7, 2023.

Suski, K. J., Hill, T. C. J., Levin, E. J. T., Miller, A., DeMott, P. J., and Kreidenweis, S. M.: Agricultural harvesting emissions of ice-nucleating particles, Atmos. Chem. Phys., 18(18), 13755–13771, https://doi.org/10.5194/acp-18-13755-2018, 2018.

Sze, K. C. H., Wex, H., Hartmann, M., Skov, H., Massling, A., Villanueva, D., and Stratmann, F.: Ice-nucleating particles in northern Greenland: Annual cycles, biological contribution and parameterizations, Atmos. Chem. Phys., 23(8), 4741–4761, https://doi.org/10.5194/acp-23-4741-2023, 2023.

Tobo, Y., Adachi, K., Kawai, K., Matsui, H., Ohata, S., Oshima, N., Kondo, Y., Hermansen, O., Uchida, M., Inoue, J., and Koike, M.: Surface warming in Svalbard may have led to increases in highly active ice-nucleating particles, Commun. Earth Environ., 5(1), 516, https://doi.org/10.1038/s43247-024-01677-0, 2024.

Tobo, Y., DeMott, P. J., Hill, T. C. J., Prenni, A. J., Swoboda-Colberg, N. G., Franc, G. D., and Kreidenweis, S. M.: Organic matter matters for ice nuclei of agricultural soil origin, Atmos. Chem. Phys., 14(16), 8521–8531. https://doi.org/10.5194/acp-14-8521-2014, 2014.